

Selective Oxidation of CO in the Presence of Hydrogen on CuO/CeO₂ Catalysts Modified with Fe and Ni Oxides

A. A. Firsova, A. N. Il'ichev, T. I. Khomenko, L. V. Gorobinskii, Yu. V. Maksimov,
I. P. Suzdalev, and V. N. Korchak

Semenov Institute of Chemical Physics, Russian Academy of Sciences, Moscow, 117977 Russia

E-mail: korchak@center.chph.ras.ru

Received December 12, 2005

Abstract—The selective oxidation of CO in the presence of hydrogen on CuO/CeO₂ systems containing Fe and Ni oxides as promoters was studied. The catalysts containing 1–5 wt % CuO and 1–2.5 wt % Fe₂O₃ supported on CeO₂ and the CuO/CeO₂ systems containing 1–2.5 wt % NiO were synthesized, and their catalytic activity as a function of temperature was determined. It was found that the additives of Fe and Ni oxides increased the activity of the CuO/CeO₂ catalysts with a low concentration of CuO. In this case, the conversion of CO at 150°C approached 100%. At the same time, these additives had no effect on the activity of the CuO/CeO₂ systems at a CuO concentration of 5 wt % or higher, which exhibited an initially high activity in the above temperature region. The forms of CO adsorption and the amounts of active sites for CO adsorption and oxidation were studied using temperature-programmed desorption. It was found that the introduction of Fe and Ni additives in a certain preparation procedure facilitated the formation of an additional amount of active centers associated with CuO. Data on the temperature-programmed reduction of samples (the amount of absorbed hydrogen and the maximum temperature of hydrogen absorption) suggested the interaction of all catalyst components, and the magnitude of this interaction depended on the sample preparation procedure. With the use of Mössbauer spectroscopy, it was found that the procedure of iron oxide introduction into the CuO/CeO₂ system was responsible for the electron–ion interactions of catalyst components and the reaction mixture.

DOI: 10.1134/S0023158407020139

INTRODUCTION

The development of high-efficiency fuel cells with the use of hydrogen as a feed is a goal for the near future [1]. Commercial hydrogen, which is mainly produced from natural gas or methanol, contains 0.5–2% CO after additional purification. A gas mixture even with these low concentrations of CO cannot be used in flow cells with electrolytic polymer membranes containing supported platinum because of its high sensitivity to CO traces. In this connection, the low-temperature selective oxidation of CO in mixtures with an excess of hydrogen is a process of the greatest current interest for the production of fuel with a CO concentration lower than 10 ppm. Systems prepared by supporting platinum-group metals onto aluminum oxide or zeolites [2–4] or gold onto various metal oxides [5–7] were proposed as catalysts for this reaction. However, catalysts prepared by supporting copper oxide onto CeO₂ were found to be most active and selective at lower temperatures [8, 9]. It was hypothesized [10–13] that the high activity of the CuO/CeO₂ catalysts was associated with a special interfacial interaction between two oxides; as a consequence of this interaction, oxygen vacancies as active centers for CO oxidation were readily generated. There are published data on the dependence of catalytic activity and process selectivity on copper oxide concentration on the surface of CeO₂.

Thus, according to Kim and Cha [14], on an 8 wt % CuO/CeO₂ catalyst, the conversion of CO was >99% at 50–90% selectivity over the temperature range 120–190°C (1 vol % CO; 0.5 vol % O₂). Previously [15], we experimentally found that, as the CuO content was increased from 0.5 to 6 wt %, not only did the conversion of CO increase, but the temperature (T_{\max}) at which a maximum conversion was reached also decreased. The systems containing 5–6 wt % CuO/CeO₂ exhibited a CO conversion of >99% over the temperature region 120–150°C (1 vol % CO; 1 vol % O₂). The conversion of CO decreased as the concentration of CuO on the catalyst surface was increased.

To increase the selectivity of CO oxidation in the presence of H₂, an important task is to extend the temperature range of the reaction with a maximum conversion (T_{\max}) toward low temperatures. This is associated with a decrease in the conversion of CO at temperatures higher than 160°C and the onset of H₂ oxidation [15]. The oxidation of CO is an exothermic reaction, and the temperature is difficult to control over a narrow range of T_{\max} because of the possible heating of the system with the predominant oxidation of H₂. To solve this problem, we synthesized and characterized the CuO/CeO₂ systems with the additives of iron and nickel oxides, which actively participate in redox processes to change the catalytic characteristics of the samples.

With the use of temperature-programmed reduction (TPR) with hydrogen, temperature-programmed desorption (TPD) of CO, and Mössbauer spectroscopy, we studied the effects of Fe and Ni oxides on the catalytic properties of the CuO/CeO₂ system. For this purpose, we used samples with both maximum activities (5 wt % CuO) and intermediate activities (1–2.5 wt % CuO).

EXPERIMENTAL

Preparation of Supported Catalysts

The following three types of samples were prepared and characterized in this study: (1) the individual oxides CuO, Fe₂O₃, and NiO supported on CeO₂; (2) the CuO–CeO₂ catalysts modified with iron and nickel oxides, which were prepared by the successive impregnation of cerium oxide with copper and iron nitrates and nickel acetate; and (3) copper and iron oxides or copper and nickel oxides supported in combination on CeO₂.

Cerium oxide was prepared from cerium(III) nitrate hexahydrate on heating at a rate of 7 K/min to 500°C in air followed by calcination at the specified temperature for 2 h. To prepare catalysts of the first type, copper, iron, and nickel oxides were supported by the impregnation of cerium oxide with a corresponding metal nitrate solution. Thereafter, the samples were dried at 150°C for 1 h; then, the temperature was increased to 500°C at a rate of 7 K/min, and the samples were calcined at this temperature for 1 h. In the synthesis of samples of the second type, a metal salt solution was initially applied to cerium oxide; the support was dried and calcined at 500°C. Next, a second metal salt solution was applied and the support was dried and calcined in accordance with the above procedure. The order of supporting copper and iron (or nickel) oxides was changed so that two types of samples were obtained for each particular composition. For example, in CuO/(Fe₂O₃/CeO₂), iron oxide was initially supported on CeO₂ and then copper oxide was supported. In the synthesis of the second sample, Fe₂O₃/(CuO/CeO₂), CeO₂ was impregnated with a copper salt solution, dried, and calcined; thereafter, iron oxide was supported. The catalysts of the third type were prepared by impregnating cerium oxide with a solution simultaneously containing two metal (copper and iron or copper and nickel) salts. Then, the samples were dried and calcined as described above. The specific surface areas of the samples were measured by the BET method using the low-temperature adsorption of argon. The concentrations of metal oxides supported on CeO₂ were varied from 1 to 5 wt % per gram of the catalyst.

Catalytic Activity Tests

The catalytic activity of samples in the reaction of CO oxidation with oxygen in an excess of hydrogen was tested in a flow-type system. A weighed portion of the catalyst (20 mg) was placed in a reactor (a tube

3 mm in diameter), and the reactor was purged with a reaction mixture containing 98 vol % H₂, 1% CO, and 1% O₂ at a flow rate of 40 cm³/min. The reaction products were analyzed by chromatography with the use of two columns packed with molecular sieves NaX (13 Å) and Porapak QS for separation. Katharometers were used as detectors.

Temperature-Programmed Reduction

A catalyst sample (60 mg) was placed in a reactor and calcined at 500°C in a flow of air for 1 h before the experiment. TPR was performed in a flow of a 6% H₂/Ar gas mixture at a flow rate of 100 ml/min. The heating was performed at a rate of 12 K/min over the temperature range 20–650°C. The amount of absorbed hydrogen was determined from TPR peak areas to within ~10%. A katharometer was used as a detector.

Temperature-Programmed Desorption

The forms of CO adsorption and the interaction of these forms with O₂ and H₂ on the CuO/CeO₂ and CuO/Fe₂O₃/CeO₂ catalysts were studied by TPD in a vacuum. A sample (50 mg) was preheated in a vacuum at 500°C for 1 h and then oxidized in oxygen for 30 min at the specified temperature and $P = 5 \times 10^2$ Pa. Thereafter, the sample was evacuated at 20°C, and the adsorption of CO was performed at the specified temperature. Then, the system was evacuated and the desorption of CO was performed by heating the sample at a rate of 12 K/min with continuous evacuation. The TPD spectrum was recorded as the dependence of changes in the desorbed gas pressure (W), which was measured using a Pirani gage, on temperature (T) [16]. The desorbed gas composition was determined using an MX-7304 mass spectrometer, and the amount of desorbed gas was measured in a repeated TPD experiment performed in a closed reactor. For these experiments, the CO, O₂, and H₂ gases were prepared in accordance with standard procedures [17]. They were supplied to a sample through a trap with liquid nitrogen in order to remove uncontrollable CO₂ and H₂O impurities.

Mössbauer Spectroscopy

The state of iron in the CuO/Fe₂O₃/CeO₂ catalysts was studied by Mössbauer spectroscopy. The Mössbauer spectra were measured on an electrodynamic instrument with a source of ⁵⁷Co in chromium. Isomer shifts (δ) were measured with respect to α -Fe. The spectra were processed using standard programs under the assumption that the line shape is Lorentzian [18].

RESULTS AND DISCUSSION

Catalytic Activity

The catalytic tests of the samples of CuO/CeO₂ and CuO/Fe₂O₃ with NiO additives were per-

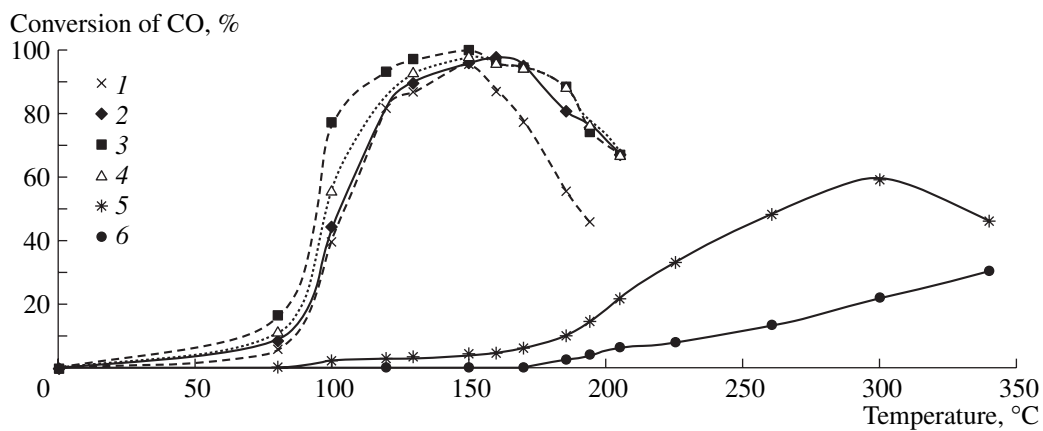


Fig. 1. Effect of the method of introducing Fe_2O_3 into the CuO/CeO_2 catalyst on the oxidation of CO in the presence of H_2 : (1) 2.5% CuO/CeO_2 (I), (2) 2.5% Fe_2O_3 /(2.5% CuO/CeO_2) (II), (3) 2.5% $\text{CuO}/(2.5\% \text{Fe}_2\text{O}_3/\text{CeO}_2$) (III), (4) (2.5% CuO + 2.5% Fe_2O_3)/ CeO_2 (IV), (5) 2.5% $\text{Fe}_2\text{O}_3/\text{CeO}_2$ (V), and (6) CeO_2 (VI).

formed over the temperature range 20–350°C. The activity of the CuO/CeO_2 samples primarily depended upon the concentration of CuO on the surface of CeO_2 . In the region 20–200°C, individual CeO_2 was inactive and a noticeable conversion of CO was detected only in the region 300–350°C: 28 or 32% at 300 or 350°C, respectively. Upon the supporting of even small amounts of CuO (around 0.5 wt %), the reaction temperature dramatically decreased and the conversion of CO noticeably increased. For this catalyst, the maximum conversion was 84% at 230°C. An increase in the concentration of CuO on the surface of CeO_2 to 1, 2.5, or 5 wt % resulted in an increase in the conversion of CO and a further decrease in the reaction temperature: 91, 95, or >99% at 165, 155, or 130°C, respectively [15]. The introduction of the iron oxide Fe_2O_3 as an additive into the catalyst changed its activity. In this case, the procedure used for the introduction of iron oxide strongly affected the degree of CO conversion. Figure 1 shows the curves of changes in the conversion of CO with temperature on the catalyst 2.5% CuO/CeO_2 (I) and the following iron-modified catalysts: 2.5% Fe_2O_3 /(2.5% CuO/CeO_2) (II), in which iron oxide was supported onto a sample of I; 2.5% $\text{CuO}/(2.5\% \text{Fe}_2\text{O}_3/\text{CeO}_2$) (III), in which iron oxide was initially applied to CeO_2 followed by drying and calcination and then copper oxide was added; (2.5% CuO + 2.5% Fe_2O_3)/ CeO_2 (IV), in which copper and iron oxides were simultaneously supported onto CeO_2 from a solution; 2.5% $\text{Fe}_2\text{O}_3/\text{CeO}_2$ (V), and CeO_2 (VI). As can be seen in Fig. 1, the sample of V was inactive and the conversion of CO reached 50% only at 300°C. Nevertheless, the supporting of iron oxide on CeO_2 improved the catalytic properties of the latter. A comparison of curves 2–4 with I shows that the addition of iron oxide to the 2.5% CuO/CeO_2 catalyst increased the activity of the samples: the conversion of CO on catalysts II and IV reached 97% at 150°C, and the conversion of CO on catalyst III was >99% at the same tem-

perature, as compared with 95% at 155°C in the absence of iron oxide. Moreover, in the region of high temperatures (160–200°C), the conversion of CO on $\text{CuO}/\text{Fe}_2\text{O}_3/\text{CeO}_2$ catalysts was noticeably higher than that on the sample of CuO/CeO_2 . In the region of low temperatures (80–120°C), the conversion of CO only on the sample of III was 10–15% higher than that on catalysts I, II, and IV. Note that the supporting of the CuO , Fe_2O_3 , and NiO oxides onto the surface of CeO_2 had an insignificant effect on the specific surface area. Thus, the specific surface area of CeO_2 was 54 m^2/g , whereas the specific surface areas of the $\text{CuO}/\text{Fe}_2\text{O}_3/\text{CeO}_2$ and $\text{CuO}/\text{NiO}/\text{CeO}_2$ catalysts lay in the range 50–56 m^2/g .

Thus, catalyst III, which was prepared by the successive supporting of iron oxide and then copper oxide on CeO_2 , exhibited the widest temperature range of CO oxidation with a maximum conversion of >99%. The activity of this catalyst was comparable with the maximum catalytic activity of a sample of 5–6 wt % CuO/CeO_2 [15].

The conversion of O_2 on the samples of I–IV was described by curves analogous to the curves of CO conversion (Fig. 2a). A maximum conversion of O_2 on these catalysts was observed at 140–160°C, where the conversion of CO also reached a maximum and was equal to 93–95%. On the catalysts 2.5% $\text{Fe}_2\text{O}_3/\text{CeO}_2$ (V) and CeO_2 (VI), the conversion of O_2 in the temperature region 140–160°C was insignificant and it increased to 78% on a sample of V only as the temperature was increased to 300°C or to 30% on a sample of VI at 350°C.

Figure 2b shows data on the selectivity of the process for oxygen on catalysts I–VI. The selectivity on the catalyst 2.5% CuO/CeO_2 (I) over the temperature region 80–190°C was 40–52% (curve 1). On the addition of iron oxide to this sample (catalysts II–IV), the selectivity increased and reached maximum values of

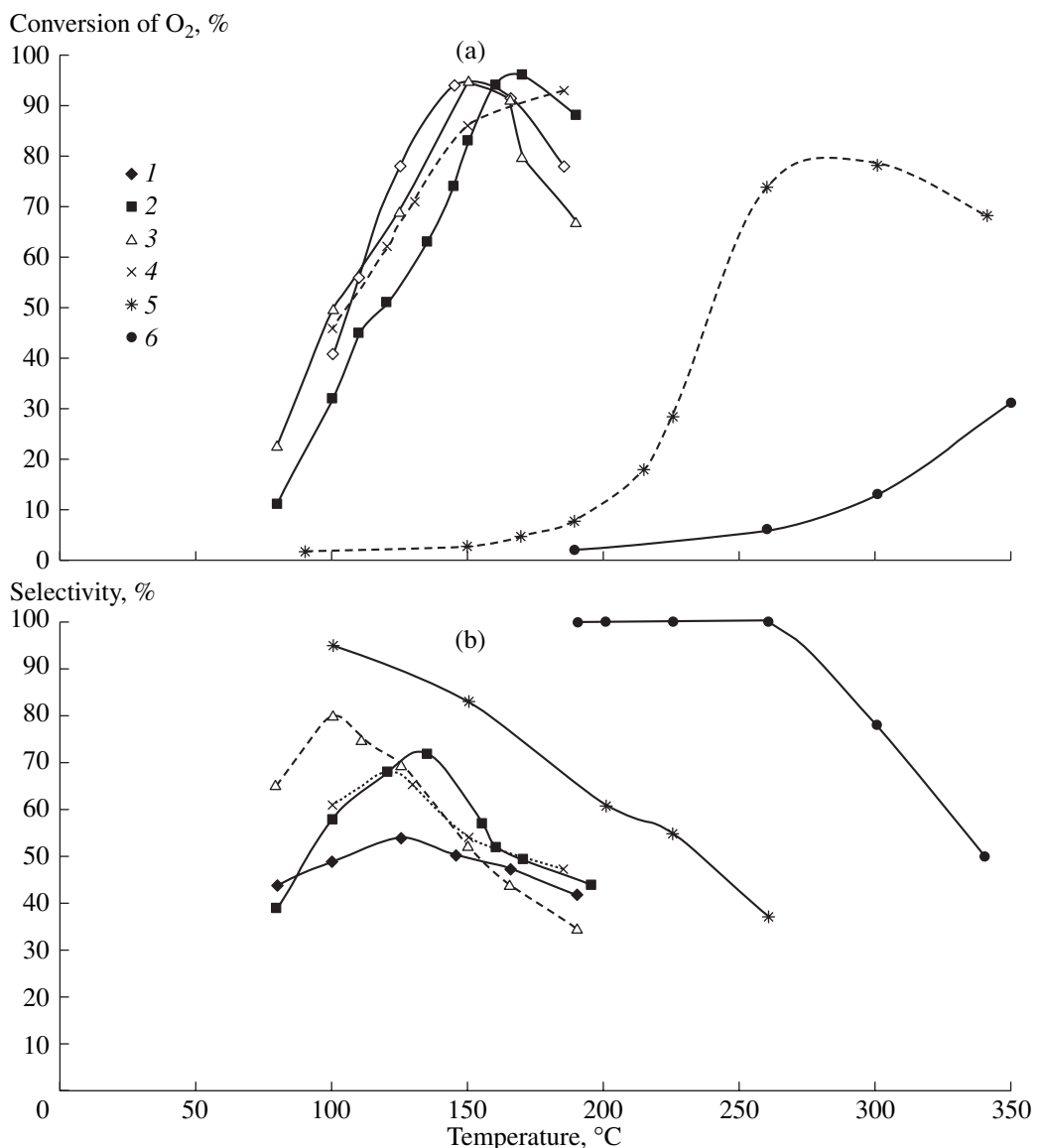


Fig. 2. (a) Conversion of O₂ and (b) process selectivity on the following catalysts: (1) 2.5% CuO/CeO₂ (I), (2) 2.5% Fe₂O₃/(2.5% CuO/CeO₂) (II), (3) 2.5% CuO/(2.5% Fe₂O₃/CeO₂) (III), (4) (2.5% CuO + 2.5% Fe₂O₃)/CeO₂ (IV), (5) 2.5% Fe₂O₃/CeO₂ (V), and (6) CeO₂ (VI).

58, 80, and 61% at 100°C on the catalysts 2.5% Fe₂O₃/(2.5% CuO/CeO₂), 2.5% CuO/(2.5% Fe₂O₃/CeO₂), and 2.5% (CuO + Fe₂O₃)/CeO₂, respectively. The selectivity decreased with temperature, and its value was no higher than 50–52% in the range 140–160°C (the region of maximum CO conversion on the samples of **II–IV**).

Thus, upon the introduction of iron oxide into the CuO/CeO₂ system, not only the conversion of CO in the region of low temperatures (100°C) but also the process selectivity increased, particularly on catalyst **III**.

Figure 3 shows the results of a study of the catalytic activity of samples containing 1 and 2.5% CuO supported on CeO₂ and CeO₂ containing 2.5% Fe₂O₃ (cat-

alyst **VII**: 1% CuO/CeO₂; catalyst **VIII**: 1% CuO/(2.5% Fe₂O₃/CeO₂)) in the reaction of CO oxidation. A decrease in the concentration of CuO in the catalysts from 2.5 (**I**) to 1% (**VII**) (curves 1 and 2) resulted in a decrease in the conversion of CO from 95 to 88% and an increase in the maximum conversion temperature from 155 to 165°C [15]. The conversion of CO on CuO/(2.5% Fe₂O₃/CeO₂) samples containing either 1 (**VIII**) or 2.5 wt % CuO (**III**) (curves 3 and 4) was higher than 99%; for both of the samples, T_{\max} was the same (150°C) and curves 3 and 4 in Fig. 3 practically coincided. As can be seen in Fig. 3, the range of T_{\max} also extended toward both low and high temperatures.

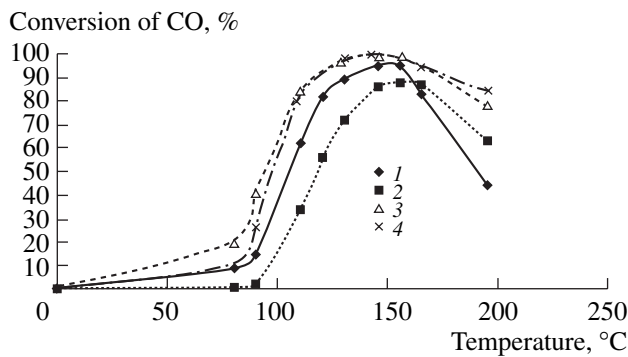


Fig. 3. Effect of the addition of Fe_2O_3 to the CuO/CeO_2 catalyst on the conversion of CO on the following samples: (I) 2.5% CuO/CeO_2 , (II) 1% CuO/CeO_2 (VII), (3) 2.5% $\text{CuO}/(2.5\% \text{Fe}_2\text{O}_3/\text{CeO}_2)$ (III), and (4) 1% $\text{CuO}/(2.5\% \text{Fe}_2\text{O}_3/\text{CeO}_2)$ (VIII).

Upon the introduction of NiO into the CuO/CeO_2 catalyst, the activity also increased. However, dissimilarities from the samples containing Fe_2O_3 were observed in this case. The conversion of CO on the samples of $\text{CuO}/(2.5\% \text{NiO}/\text{CeO}_2)$ containing either 1% CuO (IX) or 2.5% CuO (X) increased upon the introduction of nickel oxide from 88% (VII) to 98% (IX) or from 95% (I) to 99% (X), respectively (Fig. 4). A maximum conversion of CO on the samples with and without nickel oxide was reached at equal values of T_{\max} ; in the low-temperature region (see Fig. 4), curves 1 and 4, as well as 2 and 3, coincide, whereas the effect was absent from the high-temperature region (after T_{\max}). The decrease of the activities of catalysts IX and X, which contained a NiO constituent, in the high-temperature region occurred much more slowly than that of catalysts I and VII.

Temperature-Programmed Desorption

The CO and CO_2 adsorption species formed upon the adsorption of CO on CuO/CeO_2 and $\text{CuO}/\text{Fe}_2\text{O}_3/\text{CeO}_2$ catalysts were studied by TPD. Figure 5 shows spectrum 1, which was obtained after the adsorption of CO ($P = 1 \times 10^3$ Pa; $t = 10$ min) on a sample of 5% CuO/CeO_2 at room temperature. The catalyst was preheated at $T = 500^\circ\text{C}$ in a vacuum for 1 h and then oxidized with oxygen at $P = 5 \times 10^2$ Pa for 30 min at the specified temperature and evacuated at 20°C (experiment 1). Spectrum 1 exhibits three maxima. In the region of the first maximum at $T = 100^\circ\text{C}$, the desorption of CO mainly occurred; the desorption of CO_2 (70%) and CO (30%) or only CO_2 occurred in the region of the second maximum at 160 or at 240°C , respectively. The total amounts of desorbed CO and CO_2 were 4.6×10^{19} and $6.6 \times 10^{18} \text{ g}^{-1}$, respectively. It is likely that the desorption of CO at 100 and 160°C was related to the decomposition of two types of $\text{CO}-\text{Cu}^+$ carbonyl complexes [8]. The desorption of CO_2 at

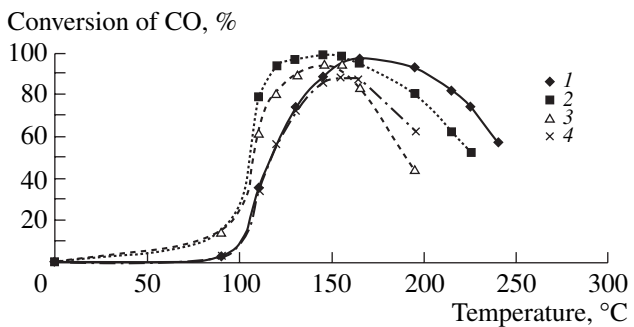


Fig. 4. Effect of the addition of NiO to the CuO/CeO_2 catalyst on the conversion of CO in the presence of hydrogen: (I) 1% $\text{CuO}/(2.5\% \text{NiO}/\text{CeO}_2)$ (IX), (2) 2.5% $\text{CuO}/(2.5\% \text{NiO}/\text{CeO}_2)$ (X), (3) 2.5% CuO/CeO_2 (I), and (4) 1% CuO/CeO_2 (VII).

160 and 240°C was related to the oxidation of adsorbed CO with surface oxygen and the decomposition of surface carbonates, respectively. To determine the degree of sample reduction as the result of the TPD of CO (experiment 1), we performed repeated adsorption of CO at 20°C followed by desorption (spectrum 2). A comparison between spectra 1 and 2 indicates that, after the repeated adsorption of CO, the amount of carbonyl and carbonate complexes was half as much as that on the oxidized surface, whereas the amount of CO_2 at 160°C decreased by a factor of 4. Evidently, both the number of CO adsorption sites and the amount of active surface oxygen, which is capable of oxidizing adsorbed CO to CO_2 , decreased as a result of the TPD of CO from the catalyst surface (experiment 1). The initial TPD spectrum of CO was restored upon the adsorption of oxygen on the catalyst surface. Thus, after the repeated adsorption of CO (spectrum 2), the sample was treated with oxygen ($P_{\text{O}_2} = 5 \times 10^2$ Pa; $T = 20^\circ\text{C}$;

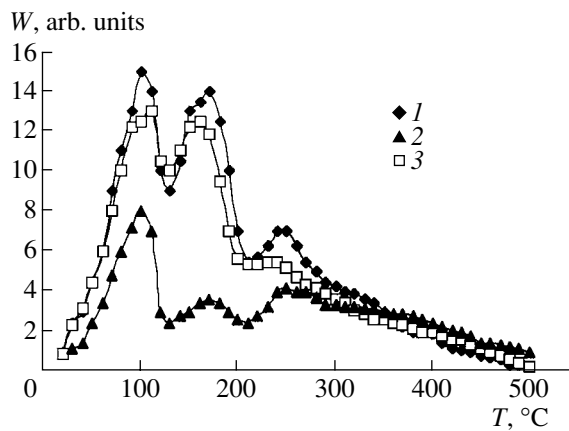


Fig. 5. TPD spectra after the adsorption of CO on 5% CuO/CeO_2 at 20°C : (I) oxidized sample, (2) sample on which CO is adsorbed after run 1, and (3) sample treated with oxygen after another CO adsorption run.

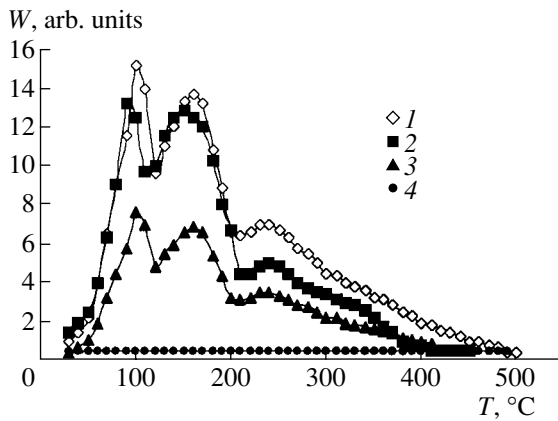


Fig. 6. TPD spectra after the adsorption of CO on oxidized samples: (1) 5% CuO/CeO₂, (2) 2.5% CuO/(2.5% Fe₂O₃/CeO₂), (3) 2.5% Fe₂O₃/(2.5% CuO/CeO₂), and (4) 2.5% Fe₂O₃/CeO₂.

$t = 10$ min) and then evacuated, and the adsorption and TPD of CO were performed once again (spectrum 3). This spectrum exhibited three maxima in the region 50–200°C; these maxima coincided with spectrum 1 in terms of temperature and intensity. Consequently, the CO adsorption sites and the surface forms of active oxygen, which were consumed in the oxidation of CO to CO₂, were regenerated upon the adsorption of O₂ even at room temperature.

A comparison between the TPD spectra obtained after the adsorption of CO ($P = 1 \times 10^3$ Pa; $t = 10$ min) at room temperature on the catalysts 5% CuO/CeO₂ and 2.5% CuO/(2.5% Fe₂O₃/CeO₂) preoxidized with oxygen (Fig. 6, spectra 1 and 2) indicated that they practically coincided. However, in the sample of 2.5% Fe₂O₃/(2.5% CuO/CeO₂), the intensity of the TPD spectrum obtained after the adsorption of CO on the oxidized catalyst under analogous conditions (Fig. 6, spectrum 3) was half as much as the intensity of spectra 1 and 2 (Fig. 6). The distribution of CO and CO₂ desorption products coincided with the distribution in spectrum 1. Carbon monoxide was not adsorbed on the sample of 2.5% Fe₂O₃/CeO₂, which contained no copper oxide (Fig. 6, spectrum 4).

Taking into account that the shapes of TPD spectra and the distributions of CO and CO₂ desorption products on catalysts **II** and **III** and on the catalyst 5% CuO/CeO₂ coincided, we can conclude that the adsorption and oxidation of CO occurred at the same sites, which were formed upon supporting copper oxide on CeO₂. This is also evidenced by the absence of CO adsorption on the sample of 2.5% Fe₂O₃/CeO₂, which was free of CuO.

However, the spectra of catalysts **II** and **III** exhibited distinctions. The amount of active sites for CO adsorption and oxidation depended upon the order of supporting the oxides CuO and Fe₂O₃ onto CeO₂. Thus, in the case of catalyst **III**, when copper oxide (2.5%

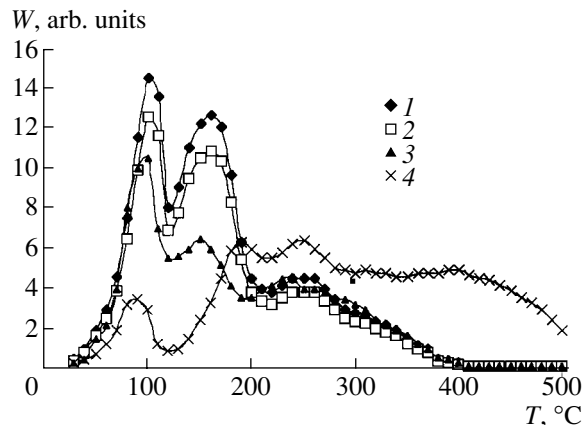


Fig. 7. TPD spectra after the adsorption of CO (1) on an oxidized sample of 2.5% CuO/(2.5% Fe₂O₃/CeO₂) at 20°C and on the above sample with adsorbed H₂ at temperatures of (2) 80, (3) 120, and (4) 160°C.

CuO) was supported onto the surface of 2.5% Fe₂O₃/CeO₂, the amount of active centers was close to the corresponding amount of centers in the catalyst 5% CuO/CeO₂, which exhibited a maximum activity. By this is meant that the preliminary supporting of Fe₂O₃ onto the surface of CeO₂ facilitated the formation of an additional amount of active centers by the interaction with CuO and an increase in the activity of catalyst **III**, as compared with that of the sample of 2.5% CuO/CeO₂. This effect was not observed in the reverse order of supporting copper and iron oxides (catalyst **II**) because the amount of active centers in catalyst **II** was half as much as that in the sample of 5% CuO/CeO₂ and corresponded to the value expected upon a decrease in the amount of supported copper oxide from 5 to 2.5 wt %, as in the catalyst 2.5% CuO/CeO₂ [15].

The effect of hydrogen adsorption on the forms of CO adsorption on catalyst **III** was studied as described below. Hydrogen was adsorbed on a sample ($P = 4 \times 10^2$ Pa; $t = 10$ min), which was preoxidized with oxygen at 500°C, at a specified temperature (T_{H_2}). After H₂ adsorption, the sample was evacuated and then cooled to room temperature; CO was adsorbed onto this sample ($P = 2 \times 10^2$ Pa; $t = 10$ min). Thereafter, TPD was performed. Figure 7 shows the TPD spectra at various values of T_{H_2} . At $T_{H_2} = 80^\circ\text{C}$, the TPD spectrum of CO (spectrum 2) differed only slightly from the TPD spectrum obtained in the initial oxidized sample (spectrum 1). An increase in T_{H_2} to 120°C resulted in a 20% decrease in the amount of CO desorbed at 100°C and a 50% decrease in the amount of CO₂ desorbed at 150°C (spectrum 3). A further increase in T_{H_2} to 160°C was accompanied by a decrease in the peak intensity of CO at 100°C by a factor of 4, whereas a peak of CO₂ at 160°C was absent from spectrum 4. In this case, the desorption of H₂O was observed in the temperature

Table 1. TPR data for CuO/CeO₂ catalysts

Sample	<i>T</i> _{max} , °C	[H ₂] × 10 ⁴ , mol/g	[H ₂] _Σ × 10 ⁴ , mol/g	[H ₂] _{excess} × 10 ⁴ , mol/g*
CeO ₂	400	—	5.3	—
	525	—		
0.25%CuO/CeO ₂	230	3.9	7.1	6.8
	350	3.2		
0.5%CuO/CeO ₂	175	2.8	6.6	6.0
	220	3.8		
1.0%CuO/CeO ₂	160	1.9	6.7	5.5
	194	4.8		
2.5%CuO/CeO ₂	127	1.7	7.2	4.6
	153	5.5		
5.0%CuO/CeO ₂	114	2.8	9.7	3.4
	150	6.9		
6.4%CuO/CeO ₂	117	3.6	12.5	4.6
	152	8.9		

* The excess of H₂ with respect to the amount of copper required for 100% reduction, considering that copper completely occurred in the state Cu²⁺.

region 150–500°C. After the TPD of CO, the catalyst remained in a reduced state; the initial activity could be restored by heating in oxygen at a reaction temperature of 80–150°C.

Thus, the preadsorption of H₂ in the region 100–160°C decreased the number of active centers for CO adsorption and oxidation. As found previously [15], hydrogen was adsorbed dissociatively and stabilized at oxygen ions, whereas it desorbed as H₂O from the catalyst surface at 270–300°C. This is consistent with the results obtained in this work.

Temperature-Programmed Reduction

The CuO/CeO₂ catalysts with different concentrations of CuO on the surface of CeO₂ and the CuO/Fe₂O₃/CeO₂ systems promoted with iron oxide were studied. Table 1 and Fig. 8 show the results of the study of the CuO/CeO₂ system. Pure CeO₂ was reduced at 400–525°C; this is consistent with published data [19, 20]. According to TPR data, the degree of reduction was 18.5%, which corresponds to the reduction of all of the Ce⁴⁺ ions to Ce³⁺ on the surface of CeO₂.

In the reduction of a sample containing copper oxide, two narrow peaks were observed in the region 100–200°C (Fig. 8, Table 1), which is much lower than the temperatures of reduction of both CeO₂ and pure CuO; this is consistent with published data [21, 22]. As can be seen in Fig. 8, high-temperature peaks due to the reduction of CeO₂ in the region 400–530°C practically disappeared from the TPR spectrum. The positions of hydrogen adsorption peaks depended on the amount of copper oxide supported onto CeO₂; the higher the concentration of CuO, the lower the temperature of copper reduction (Fig. 8). Moreover, note that the amount of hydrogen absorbed by a sample was much higher than that required for the complete reduction of supported copper from the state Cu²⁺ to Cu⁰ (Table 1). The occurrence of an excess amount of hydrogen absorbed upon the reduction of the sample in the absence of a high-temperature peak due to CeO₂ reduction allowed us to assume that the reduction of CeO₂ occurred simultaneously with the reduction of copper. Thus, TPR data suggest the occurrence of strong interactions between copper oxide and the surface oxygen vacancies of cerium oxide.

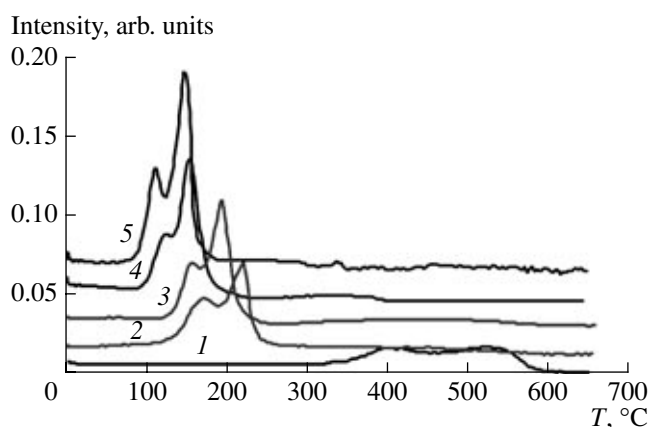


Fig. 8. TPR spectra of CuO/CeO₂ catalysts with various surface CuO contents: (1) 0, (2) 0.5, (3) 1.0, (4) 2.1, and (5) 5 wt %.

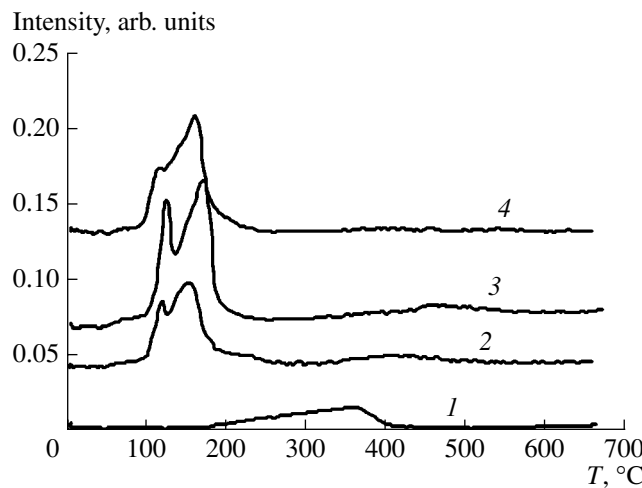


Fig. 9. TPR spectra of $\text{CuO}/\text{Fe}_2\text{O}_3/\text{CeO}_2$ catalysts prepared by various procedures: (1) 2.5% $\text{Fe}_2\text{O}_3/\text{CeO}_2$, (2) 2.5% $\text{Fe}_2\text{O}_3/(2.5\% \text{ CuO}/\text{CeO}_2)$, (3) 2.5% $\text{CuO}/(2.5\% \text{ Fe}_2\text{O}_3/\text{CeO}_2)$, and (4) (2.5% $\text{CuO} + 2.5\% \text{ Fe}_2\text{O}_3)/\text{CeO}_2$.

In the reduction of a sample of CuO/CeO_2 containing the iron oxide Fe_2O_3 in an amount equal to the weight content of copper oxide, the TPR spectrum also exhibited two narrow peaks (Fig. 9). However, a number of parameters of the spectra changed in this case (Table 2). The catalyst preparation procedure or, in more exact terms, the order of supporting copper and iron oxides onto the surface of CeO_2 , had a considerable effect on the temperature of copper reduction and the amount of absorbed hydrogen.

Mössbauer Spectroscopy

Figure 10 shows the spectra of the two iron-containing catalysts 2.5% $\text{Fe}_2\text{O}_3/(2.5\% \text{ CuO}/\text{CeO}_2)$ (II) and 2.5% $\text{CuO}/(2.5\% \text{ Fe}_2\text{O}_3/\text{CeO}_2)$ (III), which differed in the order of supporting copper and iron oxides in the

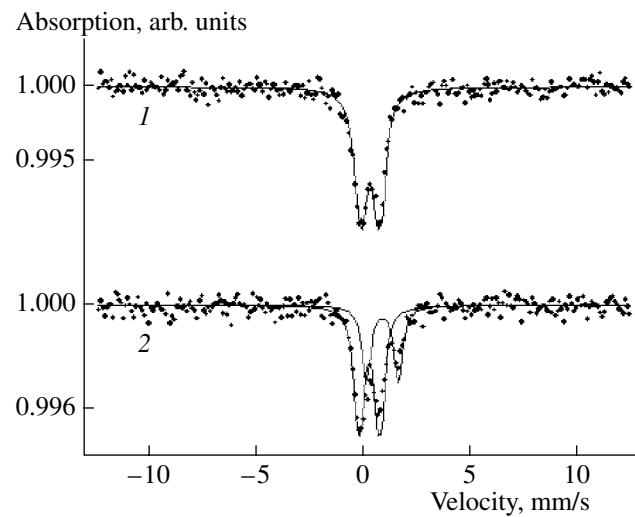


Fig. 10. Mössbauer spectra of catalysts at 300 K after the interaction with the reaction mixture: (1) 2.5% $\text{Fe}_2\text{O}_3/(2.5\% \text{ CuO}/\text{CeO}_2)$ and (2) 2.5% $\text{CuO}/(2.5\% \text{ Fe}_2\text{O}_3/\text{CeO}_2)$.

course of preparation. These spectra were measured after performing the reaction of final CO oxidation on the catalysts at 150°C for 2 h. The spectra of the samples before the reaction were analogous to spectrum 1. It is most likely that the “paramagnetic” doublet of the Fe^{3+} ion, which was observed in test systems II and III, was due to iron oxide nanoclusters with a particle size of $\sim 3\text{--}7$ nm. However, further low-temperature studies should be performed to test this hypothesis.

The Mössbauer spectra were obtained at 300°C; Table 3 summarizes the parameters of these spectra. A comparison between the spectra of catalyst II (iron oxide supported on CuO/CeO_2) before and after the reaction (Fig. 10, spectrum 2; Table 3) indicates that the state of iron remained unchanged under the action of a reaction mixture and the parameters of the spectra were

Table 2. Parameters of the TPR spectra of CuO/CeO_2 catalysts modified with Fe_2O_3

Catalyst	$T_{\max}, ^\circ\text{C}$	$[\text{H}_2] \times 10^4, \text{ mol/g}$	$[\text{H}_2]_{\Sigma} \times 10^4, \text{ mol/g}$	$[\text{H}_2]_{\text{excess}} \times 10^4, \text{ mol/g}^*$
2.5% CuO/CeO_2 (I)	127	1.7	7.2	4.0
	153	5.5		
2.5% $\text{Fe}_2\text{O}_3/(2.5\% \text{ CuO}/\text{CeO}_2)$ (II)	118	1.9	8.0	4.9
	156	6.1		
2.5% $\text{CuO}/(2.5\% \text{ Fe}_2\text{O}_3/\text{CeO}_2)$ (III)	125	3.7	12.3	9.2
	173	8.6		
(2.5% $\text{CuO} + 2.5\% \text{ Fe}_2\text{O}_3$)/ CeO_2 (IV)	118	2.0	9.8	6.6
	162	7.8		
2.5% $\text{Fe}_2\text{O}_3/\text{CeO}_2$ (V)	363	3.9	—	2.3**

*The excess of H_2 with respect to the amount required for 100% copper reduction, considering that copper completely occurred in the state Cu^{2+} .

**The excess of H_2 with respect to the amount required for the reduction of Fe_2O_3 to FeO .

Table 3. Parameters of the Mössbauer spectra of catalysts*

Catalyst	Component	δ , mm/s	Δ , mm/s	Γ , mm/s	Σ , %
2.5% Fe_2O_3 /(2.5% CuO/CeO_2), initial	Fe^{3+} , paramagnetic	0.33	0.74	0.57	100
2.5% Fe_2O_3 /(2.5% CuO/CeO_2), after reaction	Fe^{3+} , paramagnetic	0.36	0.78	0.55	100
2.5% CuO /(2.5% $\text{Fe}_2\text{O}_3/\text{CeO}_2$), initial	Fe^{3+} , paramagnetic	0.38	0.82	0.64	100
2.5% CuO /(2.5% $\text{Fe}_2\text{O}_3/\text{CeO}_2$), after reaction	Fe^{3+} , paramagnetic	0.35	0.98	0.50	69
	Fe^{2+} , paramagnetic	0.95	1.56	0.49	31

* δ is the isomer shift with respect to α -Fe; Γ is the line width; Δ is the quadrupole shift or quadrupole splitting; Σ is the relative concentration (the values of δ , Δ , and Γ are accurate to ± 0.03 mm/s; Σ is accurate to $\pm 5\%$). The internal field (H_{in}) at the iron nucleus was not determined in these spectra (the values of H_{in} are accurate to ± 0.5 T).

almost identical. However, in catalyst **III** (iron oxide was supported on CeO_2 , and copper oxide was then supported onto this system), the state of iron after the action of the reaction mixture changed considerably (Fig. 10, spectrum 2; Table 3). In the spectrum, lines due to a high-spin complex of bivalent iron in an octahedral environment lattice of oxygen ions appeared.

Thus, to summarize the experimental data, the following should be noted: On the addition of iron and nickel oxides (Fe_2O_3 and NiO) to the CuO/CeO_2 catalyst, its activity significantly changed. The sample preparation procedure for $\text{CuO}/\text{Fe}_2\text{O}_3/\text{CeO}_2$ and $\text{CuO}/\text{NiO}/\text{CeO}_2$ is of crucial importance. The catalytic activity increased only upon the successive supporting of oxides onto the surface of CeO_2 : initially Fe_2O_3 (or NiO) by impregnation with an iron (nickel) nitrate solution followed by drying and calcination at 500°C and then CuO also by the impregnation of the $\text{Fe}_2\text{O}_3/\text{CeO}_2$ (or NiO/CeO_2) system with a copper nitrate solution. The TPD data indicate that the shapes of TPD spectra and the distributions of CO and CO_2 desorption products in the samples of $\text{CuO}/\text{Fe}_2\text{O}_3/\text{CeO}_2$ prepared by different procedures coincided with those for the 5% CuO/CeO_2 sample. However, the number of active centers for CO adsorption and oxidation in the catalyst 2.5% Fe_2O_3 /(2.5% CuO/CeO_2) (**II**) was equal to that in the sample of 2.5% CuO/CeO_2 (**I**); that is, it depended on the concentration of the copper oxide CuO . The number of the above active centers in the catalyst 2.5% CuO /(2.5% $\text{Fe}_2\text{O}_3/\text{CeO}_2$) (**III**) was twice as many and corresponded to the sample of 5% CuO/CeO_2 . Evidently, an additional amount of active centers associated with CuO was formed in the preparation of catalyst **III**. Very important information, which allowed us to evaluate the effect of iron oxide on the catalytic properties of a sample of **III**, was obtained from an analysis of Mössbauer spectra. Only in the case of catalyst **III** did the interaction with a reaction mixture at 120 – 150°C result in the considerable reduction of Fe^{3+} to Fe^{2+} (Fig. 10, spectrum 2). However, recall that the sample of 2.5% $\text{Fe}_2\text{O}_3/\text{CeO}_2$ was inactive and it was reduced in hydrogen at higher temperatures in the region of 350°C (see Table 2). It is likely that a ternary oxide compound was formed upon supporting Fe_2O_3 onto the surface of CeO_2 followed by supporting CuO , and oxygen transfer

from the bulk of CeO_2 through the lattice of Fe_2O_3 to the active centers of CuO was facilitated in this ternary oxide. TPD data also suggest the occurrence of strong interactions between copper oxide and the surface oxygen vacancies of cerium oxide: the reduction temperature of copper oxide decreased with the concentration of CuO on the surface of CeO_2 (Fig. 5). An excess of hydrogen absorbed in TPR over the amount required for the reduction of Cu^{2+} to Cu^0 and the absence of a high-temperature peak due to CeO_2 reduction allowed us to conclude that this reduction of CeO_2 in the CuO/CeO_2 and $\text{CuO}/\text{Fe}_2\text{O}_3/\text{CeO}_2$ systems occurred at much lower temperatures: 120 – 160°C against 400 – 500°C (see Tables 1, 2). Moreover, the reoxidation of reduced copper on the CuO/CeO_2 and $\text{CuO}/\text{Fe}_2\text{O}_3/\text{CeO}_2$ systems readily occurred at room temperature; this reoxidation is impossible in individual copper. An increase in the number of active centers for CO adsorption and oxidation (according to Il'ichev et al. [15], Cu_2O clusters are these active centers) on catalyst **III** (according to TPD data) can be due to a decrease in the size of these clusters because of the specific interaction of CuO clusters with Fe_2O_3 clusters on supporting onto $\text{Fe}_2\text{O}_3/\text{CeO}_2$. This conclusion was also supported by data on the catalytic properties of a sample of 1% CuO /(2.5% $\text{Fe}_2\text{O}_3/\text{CeO}_2$) (see Fig. 3). Although the CuO content decreased by a factor of 2.5, as compared with that of a sample of **III**, the conversion of CO and T_{max} were practically equal on both of the samples. At the same time, as found previously [15], the activity of CuO/CeO_2 catalysts in the absence of Fe_2O_3 dramatically decreased with decreasing CuO concentration on the surface of CeO_2 .

Analogous considerations can be given to the catalysts containing NiO . The introduction of Fe_2O_3 and NiO additives into the CuO/CeO_2 system extended the temperature range of maximum CO conversion and dramatically increased the conversion of CO in the presence of H_2 by decreasing the CuO content of the CuO/CeO_2 catalyst to 1 wt %.

REFERENCES

1. Kahlich, M.J., Gasteiger, H.A., and Behm, R.J., *J. Catal.*, 1997, vol. 171, p. 93.

2. Liu, W. and Flutzani-Stefanopoulos, M., *J. Catal.*, 1995, vol. 153, p. 304.
3. Liu, W. and Flutzani-Stefanopoulos, M., *J. Catal.*, 1995, vol. 153, p. 317.
4. Avgoropoulos, G., Ioannides, T., Matralis, H., Baatista, J., and Hocevar, S., *Catal. Lett.*, 2001, vol. 73, p. 33.
5. Bethke, G.K. and Kung, H.H., *Appl. Catal.*, A, 2000, vols. 194/195, p. 43.
6. Torres Sanchez, R.M., Ueda, A., Tanaka, K., and Haruta, M., *J. Catal.*, 1997, vol. 168, p. 125.
7. Kahlisch, M.J., Gasteiger, H.A., and Behm, R.J., *J. Catal.*, 1999, vol. 182, p. 430.
8. Matinez-Arias, A., Fernandez-Garcia, M., Galvez, O., Coronado, J.M., Aderson, J.A., Conesa, J.C., Soria, J., and Munuera, G., *J. Catal.*, 2000, vol. 195, p. 207.
9. Sedmak, G., Hocevar, S., and Levec, J., *J. Catal.*, 2003, vol. 213, p. 135.
10. Wang, J.B., Shih, W.-H., and Huang, T.J., *Appl. Catal.*, A, 2000, vol. 203, p. 9.
11. Dow, W.P. and Huang, T.J., *J. Catal.*, 1996, vol. 160, p. 155.
12. Silver, R.G., Hou, C.J., and Eckerd, J.G., *J. Catal.*, 1989, vol. 118, p. 400.
13. Dilara, P.A. and Vohs, J.M., *J. Phys. Chem.*, 1993, vol. 97, p. 12919.
14. Kim, D.H. and Cha, J.E., *Proc. 9th APCChE Congr.*, 2002, p. 9.
15. Il'ichev, A.N., Firsova, A.A., and Korchak, V.N., *Kinet. Katal.*, 2006, vol. 47, no. 4, p. 602 [*Kinet. Catal.* (Engl. Transl.), vol. 47, no. 4, p. 585].
16. Tret'yakov, I.I., Shub, B.R., and Sklyarov, A.V., *Zh. Fiz. Khim.*, 1970, vol. 44, p. 2112.
17. *Handbuch der preparativen anorganischen Chemie*, von Brauer, G., Ed., Stuttgart: Ferdinand Enke, 1981.
18. Maksimov, Yu.V., Suzdalev, I.P., Khomenko, T.I., and Kadushin, A.A., *Hyperfine Interact.*, 1990, vol. 57, p. 1987.
19. Hu, Y., Dong, L., Wang, J., Ding, W., and Chen, Y., *J. Mol. Catal. A.: Chem.*, 2000, vol. 162, p. 307.
20. Xiaoyuan, J., Guanglie, L., Renxian, Z., Jianxin, M., Yu, Ch., and Xiaoming, Z., *Appl. Surf. Sci.*, 2001, vol. 173, p. 208.
21. Skarman, B., Grandjean, D., Benfield, R.E., Hinz, A., Andersson, A., and Wallenberg, L.R., *J. Catal.*, 2002, vol. 211, p. 119.
22. Tang, X., Zhang, B., Li, Y., Xu, Y., Xin, Q., and Shen, W., *Catal. Today*, 2004, vols. 93–95, p. 191.